Journal of Mammary Gland Biology and Neoplasia (2018) 23:109–123
https://doi.org/10.1007/s10911-018-9398-y

cIAP2 Is an Independent Signaling and Survival Factor during Mammary Lactational Involution and Tumorigenesis

David Carr[1] · Rosanna Lau[1,2] · Alexandra D. Hnatykiw[1] · Gwendoline C. D. Ward[1] · Manijeh Daneshmand[3] · Miguel A. Cabrita[1] · M. A. Christine Pratt[1]

Received: 26 October 2017 / Accepted: 20 May 2018 / Published online: 6 June 2018

Abstract

Cellular inhibitor of apoptosis proteins-1 and -2 (cIAP1/2) are integral to regulation of apoptosis and signaling by the tumor necrosis factor (TNF) and related family of receptors. The expression of cIAP2 in tissues is typically low and considered functionally redundant with cIAP1, however cIAP2 can be activated by a variety of cellular stresses. Members of the TNFR family and their ligands have essential roles in mammary gland biology. We have found that *cIAP2*$^{-/-}$ virgin mammary glands have reduced ductal branching and delayed lobuloalveogenesis in early pregnancy. Post-lactational involution involves two phases where the first phase is reversible and is mediated, in part, by TNFR family ligands. In *cIAP2*−/− mice mammary glands appeared engorged at mid-lactation accompanied by enhanced autophagic flux and decreased cIAP1 protein expression. Severely stretched myoepithelium was associated with BIM-EL expression and other indicators of anoikis. Within 24 h after forced or natural weaning, *cIAP2*$^{-/-}$ glands had nearly completed involution. The TNF-related weak inducer of apoptosis (Tweak) which results in degradation of cIAP1 through its receptor, Fn14, began to increase in late lactation and was significantly increased in *cIAP2*$^{-/-}$ relative to WT mice by 12 h post weaning accompanied by decreased cIAP1 protein expression. Carcinogen/progesterone-induced mammary tumorigenesis was significantly delayed in *cIAP2*$^{-/-}$ mice and tumors contained high numbers of apoptotic cells. We conclude that cIAP2 has a critical role in the mammary gland wherein it prevents rapid involution induced by milk stasis-induced stress associated with Tweak activation and contributes to the survival of mammary tumor cells.

Keywords cIAP2 · Mammary gland development · Mammary tumorigenesis

Introduction

Cells in the mammary gland undergo successive rounds of proliferation and cell death during pregnancy and involution [1]. During each estrus cycle an expansion of the epithelium generates tertiary branches and lobuloalveolar structures that then regress if pregnancy does not take place. Pregnancy results in rapid proliferation of epithelial cells mediated by progesterone stimulation of the TNFR-family member, Receptor Activator of NF-κB (RANK), to populate lobuloalveolar units that terminally differentiate near parturition to produce milk [2–4]. At weaning the gland undergoes the process of involution that takes place in two phases [5]. The first phase occurs within the first 2–3 days in mice and is thought to be a response to milk accumulation and resulting alveolar stretch [6]. This phase is reversible and involves extensive apoptosis combined with macroautophagy of the alveolar epithelial cells. In the second phase, lasting 6–8 days in mice, an irreversible structural remodeling of the mammary gland occurs [5, 6].

The first phase of involution is regulated by soluble factors belonging to the tumor necrosis factor (TNF) family including TNFα and the TNF-related weak inducer of apoptosis (Tweak) [7]. Leukemia inhibitory factor (LIF) is then secreted activating a Stat3-regulated cell death program [8]. The control of apoptosis

David Carr and Rosanna Lau contributed equally to this work.

Electronic supplementary material The online version of this article (https://doi.org/10.1007/s10911-018-9398-y) contains supplementary material, which is available to authorized users.

✉ M. A. Christine Pratt
cpratt@uottawa.ca

[1] Breast Cancer Research Lab, Department of Cellular and Molecular Medicine, University of Ottawa, 451 Smyth Road, Ottawa, ON K1H 8M5, Canada

[2] Present address: Department of Pathology, The UT M.D. Anderson Cancer Center, Houston, TX, USA

[3] Ottawa Hospital Regional Cancer Centre, Centre for Cancer Therapeutics, 3rd floor, 501 Smyth Road, Ottawa, ON K1H 8L6, Canada

and signaling through the TNFR-related receptors requires the cellular inhibitor of apoptosis proteins (cIAPs), cIAP1 and cIAP2, which possess E3 ubiquitin ligase activity. cIAP1 is often constitutively expressed and promotes the ubiquitin-mediated degradation of cIAP2 [9]. Thus, cIAP2 levels are typically low but can be induced by cellular stress signaling [10]. The cIAPs are required for the induction of canonical NF-κB (p65/RelA) following (TNFα) stimulation of the TNF receptor-1 (TNFR1) [9, 11, 12]. Consequently, loss of cIAP1/2 leads to the formation of a caspase 8-activating complex and induction of apoptosis by TNFα [11–15]. Tweak stimulation of its receptor, Fn14, results in the sequestration of the cIAPs and TNF receptor activating factors (TRAFs) at the plasma membrane, stabilizing the NF-κB inducing kinase thus activating p52/RelB NF-κB [16, 17]. Tweak also promotes the lysosomal degradation of cIAP1-TRAF2 resulting in both autocrine TNFα secretion (induced by NF-κB) and enhanced sensitivity to apoptosis in the presence of TNFα [16], thereby synergizing with TNFα in the induction of cell death. Ultimately Tweak induces the formation of a death-inducing signal complex (DISC) promoting the auto-activation of caspase 8 [17, 18].

Global knockouts for both cIAP1 and cIAP2 have been described. *cIAP1* null mice are viable and are not overtly hypersensitive to proapoptotic stimuli, however *cIAP1*$^{-/-}$ cells express markedly elevated levels of cIAP2 protein due to reduced degradation [19]. Similarly, *cIAP2*$^{-/-}$ mice are viable and fertile with no obvious phenotype, although macrophages lacking cIAP2 undergo apoptosis following challenge with lipopolysaccharide, a stimulus which normally activates cIAP2 expression in these cells [20]. Compound mutants are embryonic lethal, consistent with critical roles for cIAP1/2 that can be reciprocally compensated by either protein in most aspects of development [19].

Aside from functions in normal physiology, the involvement of the cIAPs in cancer is underscored by the frequent induction of these genes in several tumors [21, 22]. Interestingly, cIAP1/cIAP2 loss is seen in a small percentage of multiple myelomas leading to the activation of the alternative NF-κB signaling pathway in B cells [23, 24]. Given the role of cIAPs in receptor-mediated activation of NF-κB and the fact that NF-κB plays a major role in numerous cancers [25, 26], loss of cIAP1/2 expression has the potential to be associated with either cell death or tumor promotion.

The mammary lactation/involution cycle and tumorigenesis are processes that involve significant cellular stress as well as cytokines that can alter the balance of cIAP proteins. Our results illustrate key cIAP1-independent functions of cIAP2 in mammary gland biology and pathogenesis.

Results

Absence of cIAP2 Results in Reduced Branching Morphogenesis and Early Onset Rapid Involution To study the role of cIAP2 in mammary development we used the previously characterized *cIAP2*$^{-/-}$ mouse [20] in which cIAP2 is null in all cell subsets in the mammary gland. Studies have shown that XIAP and cIAP1/2 proteins are expressed at various times during pregnancy, lactation and involution [27, 28]. In agreement with others [27], using qRT-PCR analysis, we found that both cIAP1/2 transcripts were expressed in wild-type (WT) mouse virgin glands, increased during pregnancy (P) and declined during lactation (L) and after weaning (INV) (Fig. 1 a, b). Although levels were not statistically significant, *cIAP1* mRNAs trended toward higher levels throughout development in *cIAP2*$^{-/-}$ glands. Whole mount analysis and H&E-stained sections showed that virgin *cIAP2*$^{-/-}$ mouse glands appeared to have reduced ductal structures compared with control 9-week old mice. (Fig. 1 c, d). No differences in apoptotic cells were detected in *cIAP2*$^{-/-}$ and WT virgin mammary tissues (Supplemental Fig. S1). Enumeration of ductal branch points in virgin 9-week old *cIAP2*$^{-/-}$ mice compared with WT confirmed this observation (Fig. 1e, Supplemental Fig. S2A). Consistent with images in Fig. 1c, lobular areas at d12P were greater in WT mice compared to *cIAP2*$^{-/-}$ mice (Supplemental Fig. S2B). As pregnancy and lactation progress, reduced branching complexity appears to be compensated by enlargement of alveoli evident at day 18 of pregnancy (d18P) and day 7.5 of lactation (d7.5 L) in *cIAP2*$^{-/-}$ glands.

Despite these defects, cIAP2 null mice are able to lactate sufficiently to support litters based on similar mean pup weights compared with controls up until weaning (Fig. 1f). Pup weights thereafter were lower in *cIAP2*$^{-/-}$ mice indicating that cIAP2 may have a role in cell survival on a variety of tissues during rapid post-weaning growth.

Evidence for Premature Cell Detachment during Lactation, Dysfunctional Myoepithelium and Accelerated Involution in

Fig. 1 Expression of cIAP1/2 and histological comparison between cIAP2 null and wild-type mammary glands during development. RNA was harvested from mammary glands at different stages of development. **A,** qRT-PCR of cIAP1 RNA from WT and *cIAP2*$^{-/-}$ mammary glands at 9 weeks of age (virgin), 12 and 18 days of pregnancy (d12P, d18P), 7.5 days of lactation (d7.5 L) and 24 h post-weaning (24hINV). Data are means from three mouse glands performed in triplicate. Bars are S.E.M. **B,** qRT-PCR for cIAP2 in WT mammary glands at the indicated times. Data are representative of the triplicate means from three glands. Bars are S.E.M. Transcripts in A and B are normalized to β-actin mRNA. **C,** Whole mount analysis of 9-week old virgin *cIAP2*$^{-/-}$ and WT mammary glands at d12P, d18P and d7.5 L. Mammary glands were dissected and stained with hematoxylin as described in Materials and Methods. 10X objective. **D,** Hematoxylin and eosin-stained paraffin sections of mammary glands from mice at developmental stages as in C. **E,** Graph showing enumeration of branch points derived from analysis of whole mount 9 week old virgin mammary glands from *cIAP2*$^{-/-}$ and WT mice ($n = 3$ mice per genotype). **F,** Graph depicting the average mass of WT and *cIAP2*$^{-/-}$ pups at the indicated post-natal days. At least 5 pups were weighed per genotype for each time point. The arrow indicates day of weaning. Bars are S.E.M.

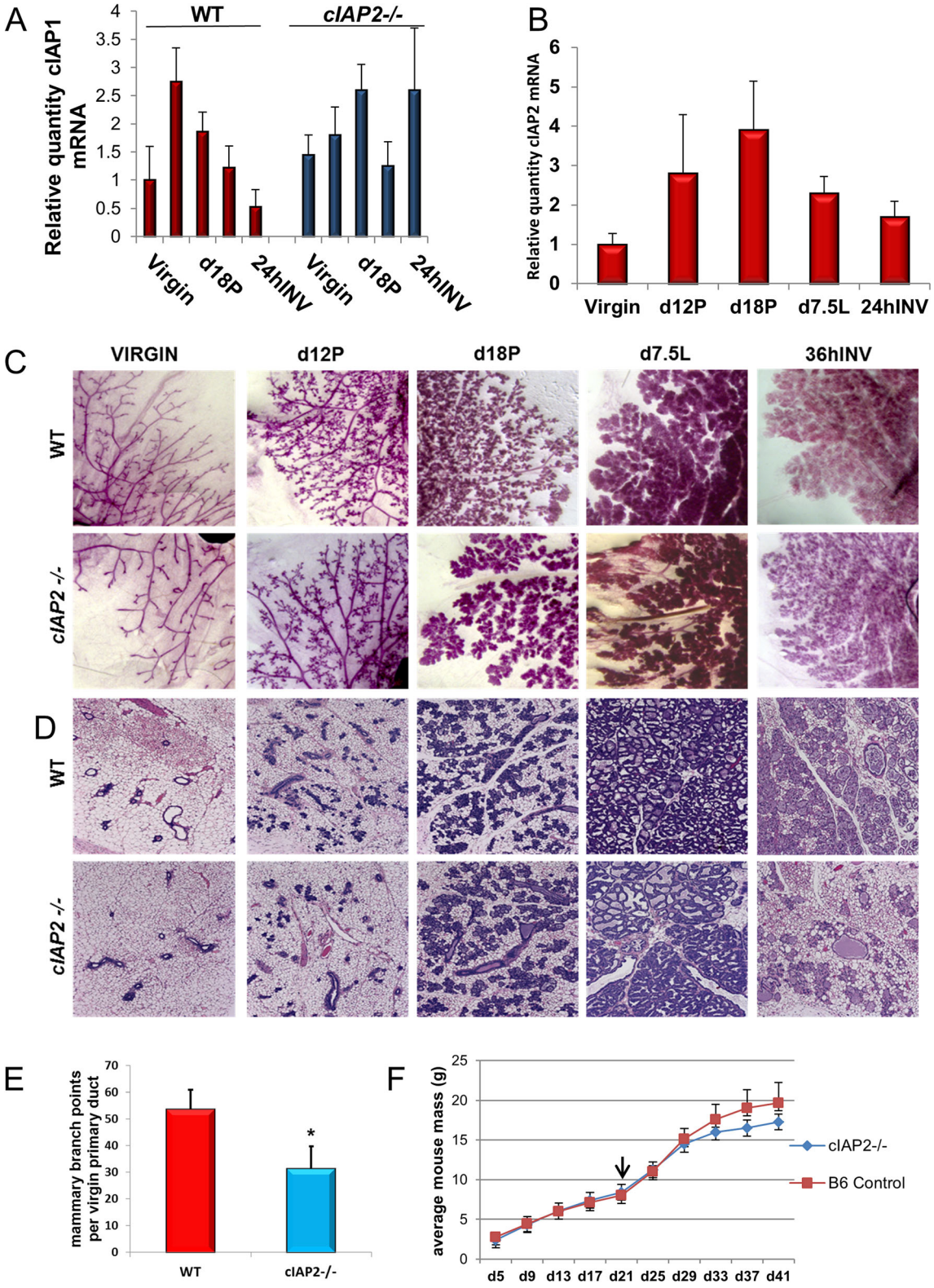

***cIAP2*$^{-/-}$ Mammary Glands** Our histological findings strongly suggest that as natural weaning approaches, the process of involution initiates prior to cessation of suckling in *cIAP2*$^{-/-}$ mammary tissue. WT mammary glands showed evidence of phase I involution with reduced alveolar size and luminal cell detachment at 36 h after weaning (36hINV). In contrast *cIAP2*$^{-/-}$ glands displayed more advanced involution at this time point where ducts and alveoli were devoid of detached cells and alveoli were collapsed (Fig. 2a). Both *cIAP2*$^{-/-}$ and WT mice produced litter sizes between 5 and 11 pups where 3/

5 litter sizes were identical in WT and *cIAP2*$^{-/-}$ mice. Since natural weaning can occur slightly earlier with smaller litters, we also examined mammary gland histology at 24 h after forced weaning at d10L. A similar acceleration of involution was observed when weaning occurred mid-lactation in *cIAP2*$^{-/-}$ mice compared to WT mice (Fig. 2b). As early as d7.5 L regions of discontinuous and bulging myoepithelial cells were evident in *cIAP2*$^{-/-}$ glands detected by smooth muscle actin IHC. This disrupted basal layer was typically associated with detached luminal cells and provides further confirmation that early and rapid involution was not a function of early natural weaning in *cIAP2*$^{-/-}$ mice. Cell death in early involution occurs through lysosomal cell death independent of classical apoptosis [29]. At 24 h after forced weaning *cIAP2*$^{-/-}$ glands contained high numbers of detached intraluminal, often binucleated death at 24 h cells which is a feature of lysosomal cell and consistent with the rapid onset of involution. Notably, the latter glands appeared highly similar to *cIAP2*$^{-/-}$ glands at d19L (Supplemental Fig. S3).

By d19L *cIAP2*$^{-/-}$ glands showed increased spacing between nuclei of stretched luminal alveolar cells, numerous detached cells and reduced cellularity compared with WT glands (Fig. 2c and Supplemental Fig. S3). Alveoli consisted of highly elongated spindle-like SMA-positive cells. In some alveolar peripheries both luminal epithelium and SMA-positive cells were undetectable. In contrast the underlying myoepithelial cells were present at both days in WT glands as a nearly continuous layer.

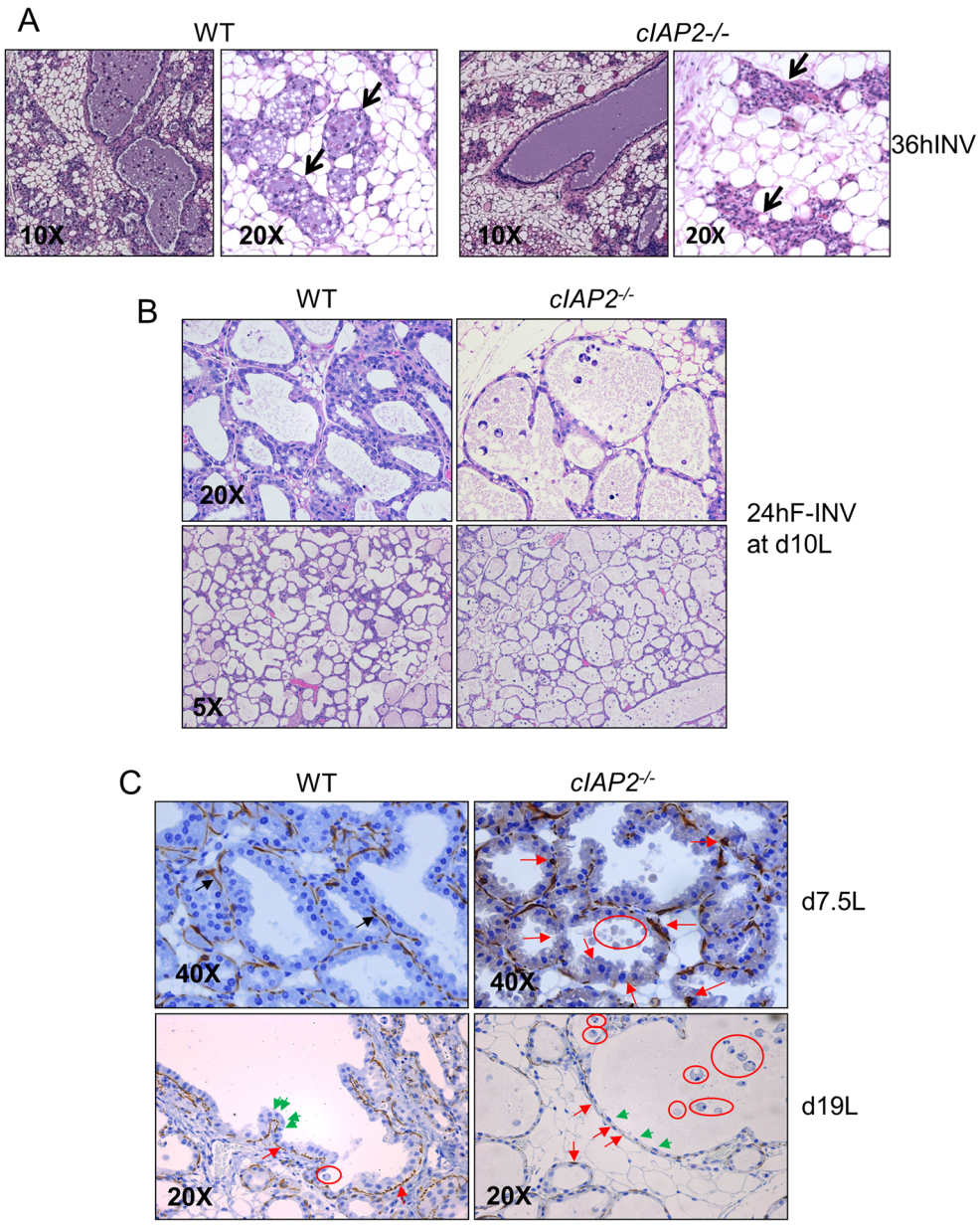

Fig. 2 Histological evidence of precocious involution in *cIAP2*$^{-/-}$ mammary glands. a, H&E sections taken from WT and *cIAP2*$^{-/-}$ mammary glands at 36 h after weaning (36hINV). Images were acquired using a 10X and 20X objective as indicated. Note the presence of detached cells in both alveolar and ductal lumens in WT but not *cIAP2*$^{-/-}$ glands. Images are representative of mammary glands from 3 mice per group. **b**, Mammary gland sections stained with H&E 24 h after forced weaning of WT and *cIAP2*$^{-/-}$ dams at d10Lwhich depict the presence of detached cells in the lumen of *cIAP2*$^{-/-}$ mammary glands and loss of cellularity. Images are representative of 3 mammary glands of each genotype. **c,** IHC to detect smooth muscle actin (SMA) expressed by myoepithelial cells in paraffin sections from d7.5 L and d19L mice. Sections were counterstained with hematoxylin. Red circles indicate dying cells typical of lysosomal cell death in phase I involution (swollen cells with two hypercondensed nuclei without membrane blebbing). Green arrows indicate luminal epithelial cells and red arrows indicate SMA-positive myoepithelial cells in WT and *cIAP2*$^{-/-}$ glands. Images are representative of 3 mammary glands at each time point per genotype

Milk stasis induces mechanical stretch on alveolar cells to trigger early events in involution [8]. Milk accumulation during lactation in *cIAP2*$^{-/-}$ mice would increase milk content in the gland. Supplemental Fig. S4 shows only a slightly increased content of β-casein in mammary glands lacking cIAP2 relative to control glands at d18P. This suggests that the early failure of myoepithelium and luminal cell detachment in *cIAP2*$^{-/-}$ glands may be due to stress associated with reduced ductal branching and volume capacitance.

***Tweak* Expression Is Dysregulated in *cIAP2*$^{-/-}$ Mammary Glands Early in Involution** Stat5 phosphorylation occurs in response to prolactin [1] and was normal in *cIAP2*$^{-/-}$ mammary glands during pregnancy and lactation (Supplemental Fig. S5). The first phase of involution is induced by cytokines including TNFα and Tweak resulting in NF-κB-mediated transcription of LIF which then activates Stat3 [8]. qRT-PCR showed that virgin cIAP2 mice trended toward production of higher levels of TNFα mRNA relative to WT mice (Fig. 3a). However, as indicated in the Methods section, virgin mice were not estrus matched, therefore we cannot rule out that differences in some gene and protein expression across different virgin mice within this study could be influenced by estrus stage. Tweak expression peaks at 12 h following forced involution in normal mice [7] which coincides with milk stasis. Consistent with this we observed an approximate 2-fold increase in Tweak mRNA at 12hINV in WT mice. In contrast, *cIAP2*$^{-/-}$ mice displayed a significant (3.5-fold) increase in Tweak mRNA at 12hINV that was further elevated at 24hINV (Fig. 3b).

Activation of the Tweak receptor, Fn14, results in internalization and degradation of cIAP1 within a multi-vesicular body [17]. We analyzed cIAP1/2 protein levels using a commercial antibody that reacts with both mouse cIAP1 and cIAP2. The amino acid sequences of murine cIAP1 and cIAP2 exhibit 69% identity and 81% similarity and have predicted molecular masses of 69.7 and 67.3 kDa respectively but can migrate inversely or be indistinguishable on SDS-PAGE [30] (and supplemental references). Notably, we detected increasing expression of cIAPs in WT glands through pregnancy and lactation which persisted until 12hINV but were then profoundly reduced by 36hINV. While cIAP1 was also increased up to d18P in *cIAP2*$^{-/-}$ mammary glands tissues, unlike WT mice, the levels declined by d7.5 L and did not increase until 36hINV (Fig. 3c). The reduction in cIAP protein beginning at d7.5 L in *cIAP2*$^{-/-}$ mammary glands combined with the morphological evidence of engorgement at this time point is suggestive of stress-induced reduction of cIAP1. The continued expression of cIAP1/2 until 12hINV in WT glands contends that cIAP1/2 protein expression is normally maintained at least at early stages of cellular stress associated with milk stasis.

The onset of involution results in the upregulation of cell death receptor components [7]. Traf2 is an integral component of TNFR superfamily signaling. Tweak also induces cathepsin-mediated lysosomal proteolysis of Traf2 [17]. Traf2 expression increased at d19L in *cIAP2*$^{-/-}$ mice (Supplemental Fig. S6). Consistent with high Tweak levels, by 24hINV Traf2 protein was undetectable.

Both cIAP1 and cIAP2 are critical components of TNFR family signaling controlling the activation of both canonical and alternative NF-κB activation (p52) by subsets of this receptor family involved in lobuloalveolar expansion [31] and involution [32]. Analysis of p52 expression in developing mammary glands during pregnancy and early lactation showed no differences between *cIAP2*$^{-/-}$ and WT glands (Fig. 3e) although *cIAP2*$^{-/-}$ virgin glands expressed a constitutive level of p52. During involution, activation of Fn14 by Tweak is predicted to activate IKKα and processing of p100 to p52 [16]. Indeed, p52 was present in d19L *cIAP2*$^{-/-}$ mammary glands but absent in WT glands at this time point (Fig. 3f). Thus *cIAP2*$^{-/-}$ mammary glands undergo accelerated involution in conjunction with persistent elevation of Tweak expression and a reduction in cIAP1 protein levels beginning at mid-lactation.

***cIAP2*$^{-/-}$ Mammary Glands Demonstrate Persistent Autophagic Flux during Lactation which Precedes Early Anoikis** In response to cell detachment, activation of autophagy normally occurs within 24–48 h of involution and contributes to the reversibility of this phase [33]. Numerous detached cells are found in the lumen of *cIAP2*$^{-/-}$ mouse alveoli and ducts as early as d7.5 L (see Fig. 2b). Loss of attachment can transiently induce autophagy as a survival mechanism. A gradual increase in the lipidated form of LC3 (LC3-II) in *cIAP2*$^{-/-}$ tissue detected from d7.5 L to 24hINV but only evident in WT glands at 24hINV (Fig. 4a). Upon detachment or changes in cell shape, epithelial cells lose integrin-mediated survival signaling resulting in a form of programmed cell death termed anoikis [34, 35]. Cell detachment from the basement membrane downregulates EGFR expression thereby reducing Erk1/2 activity [35]. Analysis of P-Erk1/2 in *cIAP2*$^{-/-}$ and WT mice showed similar activation in pregnant and lactating glands at the days shown with the exception of 24hINV where a strong reduction in P-Erk1/2 can be seen in *cIAP2*$^{-/-}$ mammary glands that was not a consequence of reduced levels of Erk1/2 (Fig. 4b). Loss of cell adhesion can result in phosphorylation of p38 which can contribute to inhibition of Erk1/2 activity [36]. Consistent with anoikis, immunoblots showed strong induction of P-p38 at d19L in both *cIAP2*$^{-/-}$ and WT glands which remained expressed at 24hINV in *cIAP2*$^{-/-}$ tissue (Fig. 4d). Interestingly, a second induction of P-p38 at 36hINVW in both mouse glands that was much stronger in *cIAP2*$^{-/-}$ tissue consistent with the massive changes in the architecture of the glands.

Another hallmark of anoikis is increased Bim-EL protein expression [37]. In matrix-attached cells

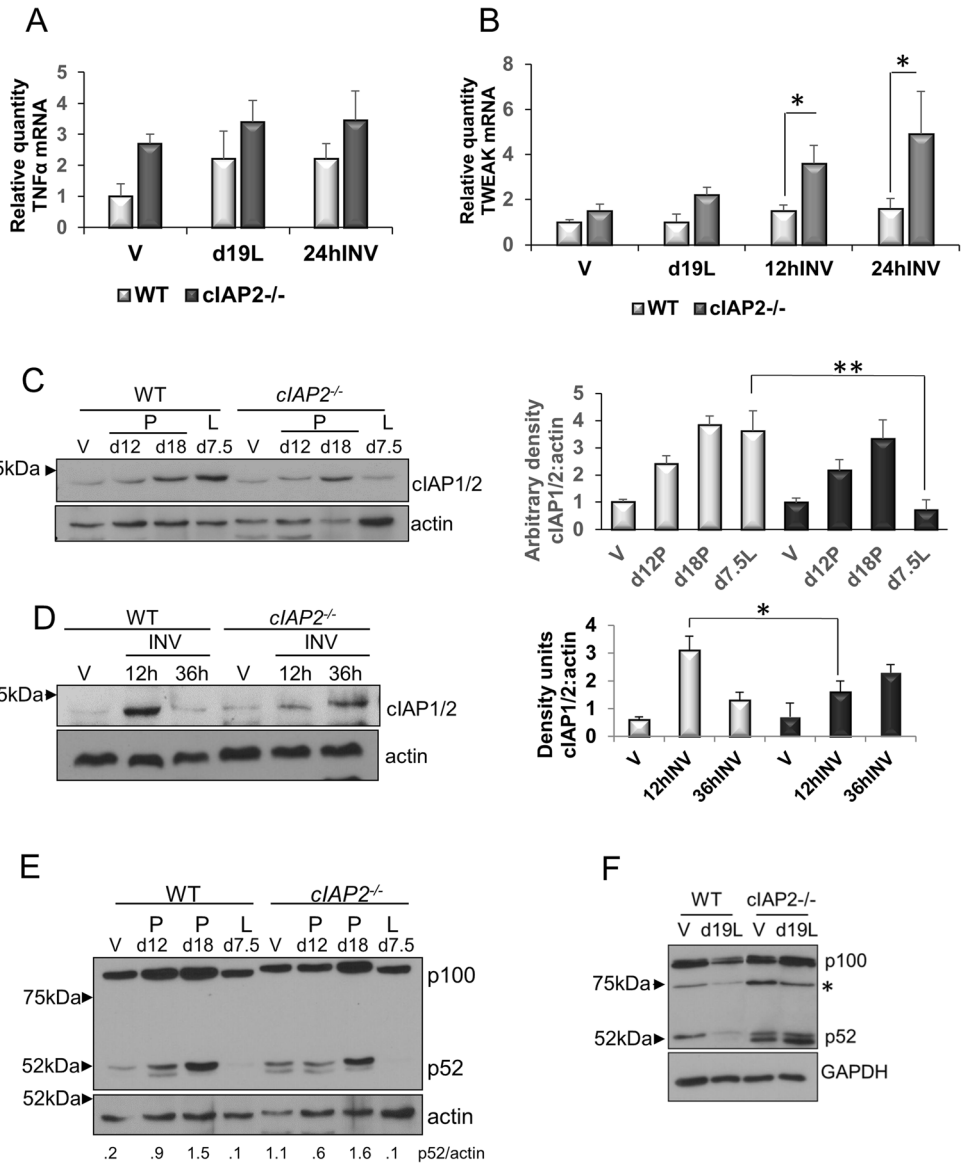

Fig. 3 Absence of cIAP2 results in hyperactivation of *Tweak* expression and amplified death signaling in vivo. qRT-PCR for **a,** T*nfα* and **b**, *Tweak* mRNA transcripts in virgin mice, 48 h prior to weaning (d19L) and 1 day post weaning (24hINV). Values shown are normalized to β-actin and are representative of triplicate values from 3 mice per time point. Bars are S.E.M. * $p < .05$, Student's t-test. **C** and D, Representative immunoblots for cIAP1/2 in virgin and lactating mammary glands. Fifteen μg of protein was immunoblotted with an antibody which detects both cIAP1 and cIAP2 mouse proteins. Vinculin was used as a loading control. Bar graphs beside the blots indicate means ± S.E.M. of densitometric values for cIAP2 relative to actin for 3 mice per time point. * $p < .05$, Student's t-test. **E** and **F** Immunoblots detecting activation of non-canonical NF-κB indicated by processing of p100 to p52 at the indicated stages of development and comparing virgin and d19L in WT and *cIAP2*$^{-/-}$ mammary glands respectively. The asterisk below p100 indicates a non-specific immunoreactive band. Numbers below are densitometry for p52/actin and are representative of determinations from 3 mice per time point

activated Erk1/2 phosphorylates Bim, targeting it for proteasomal degradation [38]. Bim is weakly expressed in WT glands at d19L and increases markedly at 24hINV. In contrast, Bim begins to increase at d7.5 L and levels are profoundly increased in *cIAP2*$^{-/-}$ glands at d19L which only decline slightly by 24hINV (Fig. 4d). Of note, in addition to cell detachment, Bim can be also be regulated through NF-κB-mediated Egr-1 expression [39]. Therefore induction of alternative NF-κB (see Fig. 3g) could also contribute to the large increase in Bim by d19L. Bim is expressed in both virgin and 36hINV *cIAP2*$^{-/-}$ glands and in WT mice as previously reported [40]. Interestingly, WT and *cIAP2*$^{-/-}$ glands showed a second increase in P-p38 at 36hINV although this was greater in *cIAP2*$^{-/-}$ compared to WT tissue (Fig. 4e). Taken together, these results suggest that cIAP2 contributes to the maintenance of the mammary epithelium in the first stages of involution in response to cellular stress and Tweak signaling.

Apoptotic Cell Death in *cIAP2*$^{-/-}$ Mammary Glands

Phosphorylated-Stat3 (P-Stat3) is a key regulator of cell death during the first phase of involution where it promotes the uptake of milk fat globules resulting in cell death due to lysosomal membrane permeabilization [41]. P-Stat3 expression in *cIAP2*$^{-/-}$ and WT mammary glands followed a similar pattern of activation where activity was strongly reduced at d7.5 L relative to pregnancy then robustly increased by 24hINV (Fig. 5a). In 2/4 WT mice we detected P-Stat3 at d19L while all *cIAP2*$^{-/-}$ mouse tissue contained P-Stat3 at this time (Fig. 5b). Most strikingly, levels of P-Stat3 were consistently higher in *cIAP2*$^{-/-}$ mice compared to controls. Stat3 activation can block the inhibitory phosphorylation of FOXO3a [42], thereby permitting the transcriptional activation of target genes such as

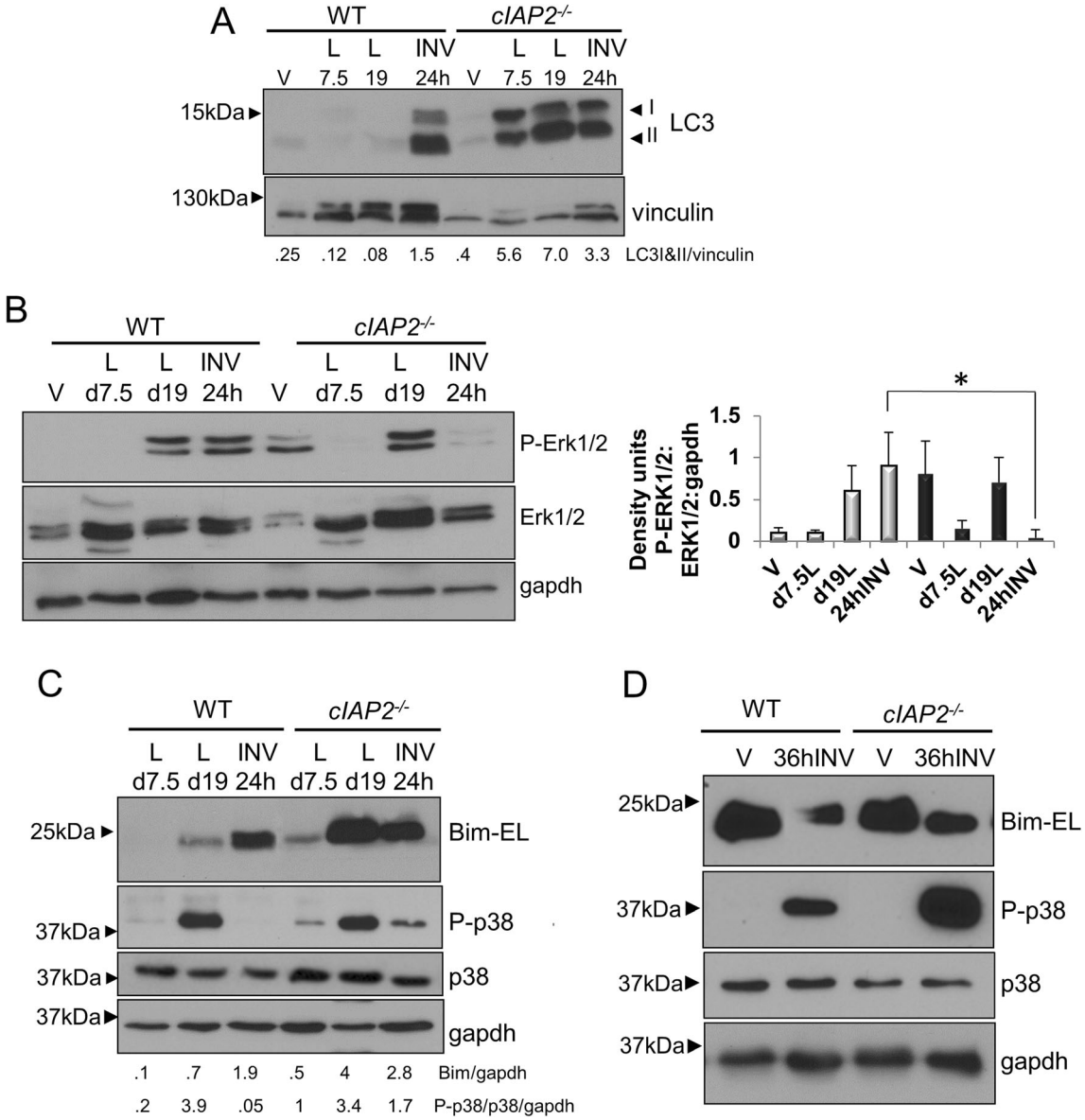

Fig. 4 Evidence for autophagy and anoikis-associated cell death signaling prior to weaning in *cIAP2*$^{-/-}$ mammary tissue. a, Detection of LC3-I and lipidated LC3-II in immunoblots of mammary gland lysates during lactation. The presence of both forms after the first week of lactation is apparent in *cIAP2*$^{-/-}$ glands. **b,** Representative immunoblots to detect phosphorylated Erk1/2 kinases in virgin glands and at the indicated time points in early and late lactation and after weaning. Twenty μg of mammary gland lysate from WT and *cIAP2*$^{-/-}$ mammary glands harvested on the indicated days were immunoblotted with anti-P-Erk1/2 and total Erk1/2. The bar graph indicates mean densitometric values from 3 mice per time point for phosphorylated proteins relative to total Erk1/2 protein and gapdh ± S.E.M. **c,** Immunoblots of P-Akt-1 and total Akt-1 in the late stage of lactation and early involution. The asterisk denotes a high mol wt non-specific band in the *cIAP2*$^{-/-}$ lane. **d,** Activation of p38 Mapk (P-p38) relative to total p38 and Bim-EL proteins detected by immunoblot at the indicated time points. **e,** Bim-EL and P-p38 expression in virgin and 36hINV mouse glands. Representative blots are shown. Numbers below are the means of densitometric values from blots of 3 mice per time point normalized as indicated

Tweak [42]. Thus the strong activation of P-Stat3 may contribute to the enhanced level of *Tweak* transcripts detected in *cIAP2*$^{-/-}$ mammary glands at 24hINV (see Fig. 4b).

During normal phase I involution, caspase activation is initially limited to detached cells and only later does it become activated in the luminal structures [32]. Stimulation of cell death by receptors in the TNFR superfamily activates caspase 8. Immunoblots for the pro-form of caspase 8 and cleaved caspase 8 in Fig. 5c show that the activated p24 cleavage product [43] was strongly detected in virgin and d19L *cIAP2*$^{-/-}$ mouse glands suggestive of constitutive death receptor-activation. Previous reports have shown that caspase 3 is not activated until day 3 of involution in WT mice [44] which is consistent with our results showing the absence of the 24 kDa cleavage product at the stages analyzed. Immunoblot to detect caspase 3 in Fig. 5d

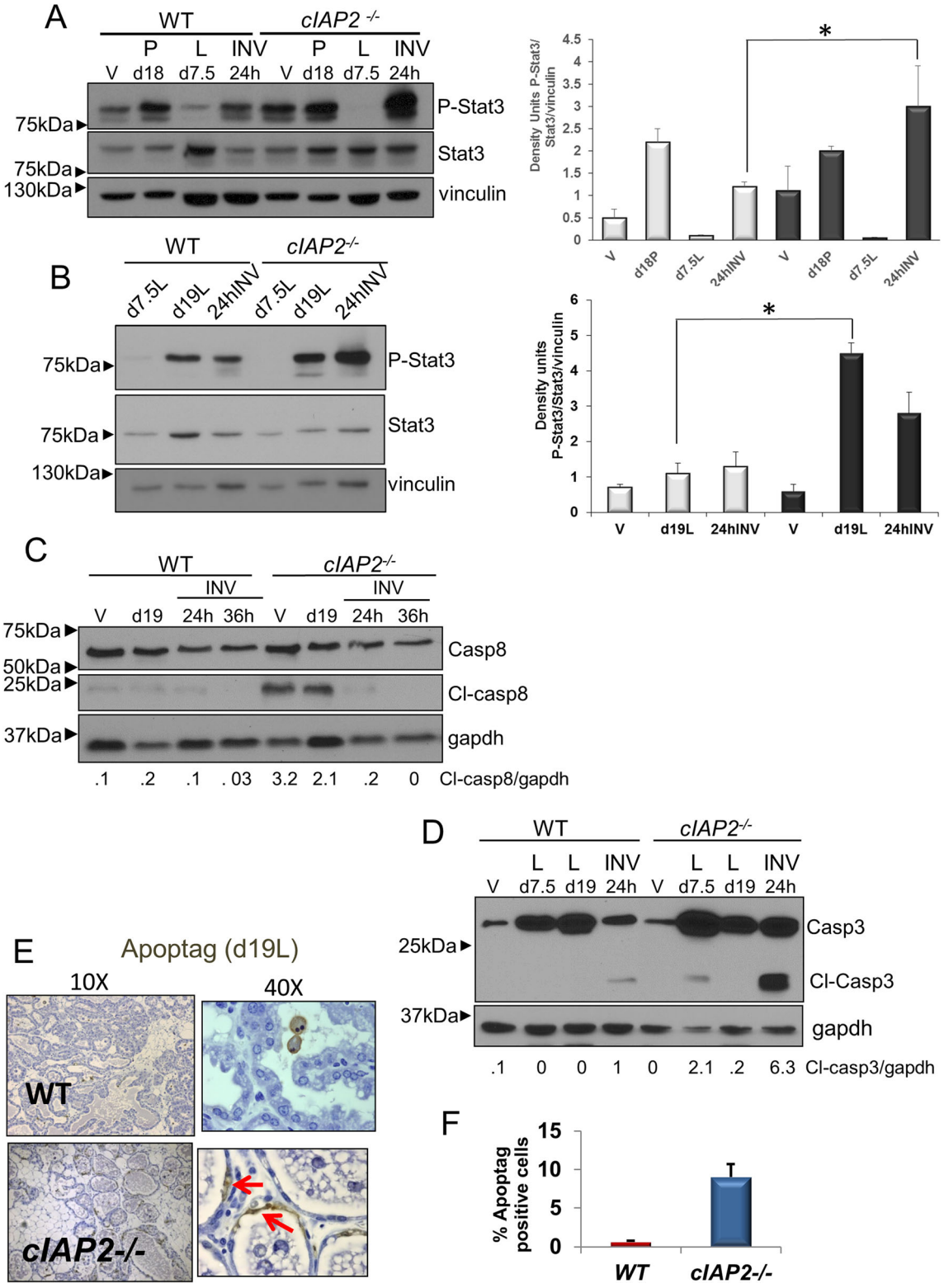

shows that cleaved caspase 3 was prematurely present in *cIAP2*$^{-/-}$ mouse glands at 24hINV compared with WT glands, consistent with large scale involution. Paraffin sections from d19L mice labeled using Apoptag to detect apoptotic cells confirmed the presence of numerous *cIAP2*$^{-/-}$ basal and luminal apoptotic cells while control glands showed apoptosis in only a subset of detached cells (Fig. 5e). Enumeration of apoptotic cells showed that a significantly greater percentage of cells were apoptotic in *cIAP2*$^{-/-}$ glands compared to control glands (Fig. 5f).

◀ **Fig. 5 Absence of cIAP2 results in accelerated mammary involution associated with precocious apoptosis. a** and **b**, Representative P-Stat3 and total Stat3 immunoblots of 20 μg of mammary gland lysate from WT and *cIAP2*$^{-/-}$ mammary glands collected at the indicated times. The bar graphs show mean densitometric quantification of phosphorylated P-Stat3 relative to Stat3 protein and vinculin from 3 mice per time point ± S.E.M. * $p < .05$ Student's t-test. Protein extracts from virgin, lactating and weaned glands immunoblotted with anti-caspase8 **(c)** and anti-caspase-3 (**d**). The 24 kDa band in C represents activated cleaved (Cl-Caspase8). The lower band in D (Cl-caspase3) indicates activated caspase3. Values below blots in C and D are means of densitometric values from blots of proteins from 3 mice per time point. **e,** Apoptag labeling of 3' DNA ends detected using alkaline peroxidase and chromogen to identify apoptotic cells in WT and *cIAP2*$^{-/-}$ mammary glands at d19L. Full images from a 10X objective and cropped 40X images are shown. The 40X image of a WT gland shows an example of the few apoptotic detached cells detected while the *cIAP2*$^{-/-}$ gland shows an example of apoptosis in the wall of cells surrounding stretched alveoli (arrows). Images are typical of Apoptag labelling in glands from 3 mice per genotype. **f,** Graph depicting the percentage of apoptotic cells in d19L WT and *cIAP2*$^{-/-}$ glands. Mean percentages were calculated based on enumeration of total labelled nuclei from 8 random 40X fields (approximately 600 cells) from 3 mice per genotype. Bars are standard deviation of apoptotic cell counts for each field. ** $p < .005$, unpaired t-test

Thus, in the absence of cIAP2, early onset involution progresses rapidly to apoptotic cell death.

Absence of cIAP2 Increases the Latency of Dimethyl-Benzanthracene (DMBA)-Induced Tumor Formation The cIAP1/2 proteins are thought to have pro-survival roles in cancer cells however the role of individual cIAPs in vivo in the process of mammary tumor formation has not been studied. Figure 6a depicts the time to tumor detection following the DMBA mammary carcinogenesis protocol [45] in WT and *cIAP2*$^{-/-}$ mice. The mean latency for *cIAP2*$^{+/+}$ mice was 93 days while that for *cIAP2*$^{-/-}$ mice was significantly longer at 127 days. Three healthy *cIAP2*$^{-/-}$ DMBA-treated mice (12.5%) never developed any palpable lesions.

High rates of cell death in the absence of cIAP2 could delay the formation of tumors. TUNEL assays on tumor sections are shown in Fig. 6b. Percentages of apoptotic cells were quantified in tumor sections from both groups of mice. Figure 6c shows that *cIAP2*$^{-/-}$ tumors contained approximately an 8-fold greater percentage of apoptotic cells compared with WT tumors. Tumor histopathologies ranged from well to poorly-differentiated adenocarcinomas. Examples are shown in Supplemental Fig. S7A. Figure 6d depicts tumor pathologies from *cIAP2*$^{-/-}$ and WT mice. Some tumors contained squamous cell regions with varying keratinization and were categorized as benign pseudoepitheliomatous hyperplasia.

cIAP2 null mice have an insertion of the β-galactosidase gene downstream of the *cIAP2* promoter [20]. Immunoblot for β-galactosidase showed the *cIAP2* promoter is activated in *cIAP2*$^{-/-}$ tumors consistent with a role for cIAP2 in tumor survival and/or signaling (Fig. 6e). Squamous hyperplasia contained almost no detectable cIAP1 or cIAP2 mRNA while cIAP2 mRNA was expressed in WT tumors (Supplemental Fig. S7B). cIAP1/2 protein levels were higher in WT tumors compared to *cIAP2*$^{-/-}$ tumors with similar histopathology which likely correlates with the combined expression of cIAP1/2 in WT tumors (Supplemental Fig. S7C). No compensatory difference in the expression of XIAP protein in WT and *cIAP2*$^{-/-}$ tumors was detected (Supplemental Fig. S8). Collectively these results indicate that cIAP2 plays a significant anti-apoptotic role in the establishment of mammary adenocarcinomas.

Discussion

Both cIAP1 and cIAP2 have similar roles in signaling through TNFR-and related family member receptors where they function as E3 ligases to regulate caspases and the activation of NF-κB and MAPK [46]. Although cIAP1 and cIAP2 are considered to be redundant in most normal cells, our analysis showed that cIAP2 has a discrete role in maintaining mammary gland integrity during lactation such that absence results in the rapid onset of involution that was nearly complete by 36hINV. The reduced ductal branching in virgin *cIAP2*$^{-/-}$ mice likely contributed to engorgement by mid-lactation. The underlying reasons for the branching deficit are not clear since the combined levels of cIAP1/2 in virgins of both genotypes appeared to be similar until mid-lactation. It is possible that the global nature of the knockout may have affected factors involved earlier in mammary development. Indeed both Tweak [47] and another TNFR-related receptor for ectodysplasin [48] participate in mammary branching. Of note, cIAP2 mRNA is also expressed in the normal human mammary epithelial stem and immature progenitor cell hierarchy (Supplemental Fig. S9) and its absence may reduce viability and or affect cytokine signaling during branching morphogenesis. The only documented phenotype in cIAP2 mice is a defect in the macrophage response to lipopolysaccharide challenge [20] which appears to be unrelated to the mammary gland phenotype described here. The presence of constitutive alternative NF-κB activity and activated caspase 8 in 9 week-old *cIAP2*$^{-/-}$ virgin mice suggests that some aspects of TNFR-family signaling may be aberrant in the absence of cIAP2 during mammary gland development. However, activation of large scale apoptosis was not evident as indicated by the lack of caspase 3 cleavage and no apparent increase in apoptotic cells in glands of *cIAP2*$^{-/-}$ virgin mice. Notably, *cIAP2*$^{-/-}$ mammary tissues demonstrated a reduction in cIAP1 protein at mid-lactation coinciding with the onset of ductal distension. Moreover, cIAP1 levels remained low in *cIAP2*$^{-/-}$ mice until 36hINV while a reduction in total cIAP proteins was only detected in WT mice after 12hINV. Together these results suggest that cIAP2 is either very low or not expressed in the normal mammary gland until milk accumulation-induced cell stress activates Tweak reducing cIAP1 protein [17] and stabilizing cIAP2 protein [9]. Thus, cIAP2 contributes to maintaining the gland during phase I

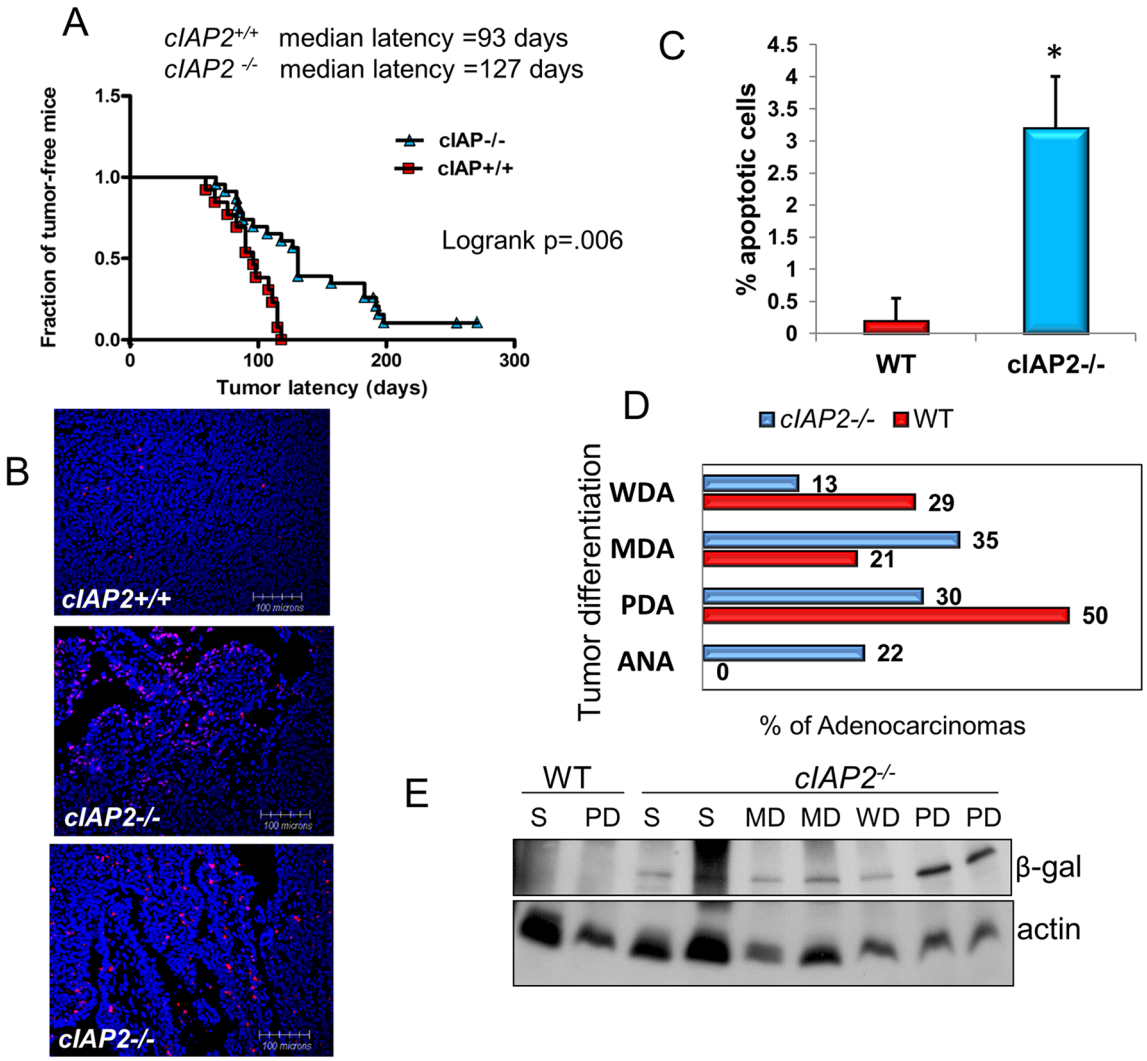

Fig. 6 Mice lacking cIAP2 develop tumors with long relative latency. **a** Kaplan-Meier analysis of tumor-free period in DMBA treated *cIAP2*$^{-/-}$ and WT mice. Animals were palpated three times weekly for lesions and latency is calculated from the final DMBA gavage. The analysis shows significantly longer latency to tumor palpation in *cIAP2*$^{-/-}$ mice compared with WT mice ($p = .006$, Log rank test), with 12% of *cIAP2*$^{-/-}$ animals remaining lesion-free. Only carcinomas were included in the analysis. **b,** TUNEL assay using Apoptag on sections of tumors derived from WT and *cIAP2*$^{-/-}$ mice. The top panel shows typical staining in a section from a *cIAP2*$^{+/+}$ adenocarcinoma. The two panels below are representative of TUNEL staining in all adenocarcinomas obtained. Bar represents 100 μm. **c,** Enumeration of apoptotic cells in tumor sections from DMBA-treated *cIAP2*$^{-/-}$ and WT mice. Three random high power fields of 300 cells were counted from each tumor section (excluding necrotic areas) and subjected to a two-tailed student's t-test (* $p < 0.05$ for both sets, Student's t-test). Tumors: DMBA-induced tumors: *cIAP2*$^{-/-}$ $n = 7$; WT $n = 6$. **d,** Graph depicting the number of lesions representing each level of tumor differentiation in WT and *cIAP2*$^{-/-}$ mice. Adenocarcinomas were classified as: WDA, well-differentiated; MDA, moderately-differentiated; PDA, poorly-differentiated; ANA, anaplastic (undifferentiated). **e,** 30μg of protein extracts from adenocarcinomas, a squamous hyperplasia (SH) from WT and *cIAP2*$^{-/-}$ mice as indicated were immunoblotted to detect β-galactosidase. Both squamous hyperplasias used for blotting contained significant inflammation

involution and, in its absence, involution proceeds rapidly. This thesis is further supported by results in other tissues such as intestinal epithelial cells where detachment induces the specific upregulation of cIAP2 which then functions to delay anoikis [49]. Importantly, the translation of cIAP2 mRNA is also promoted by stress [10, 50]. Applying this paradigm to mammary epithelium, *cIAP2*$^{-/-}$ cells would lack the response to weaning induced cellular stress and the restraint on cell death. Both Tweak signaling through Fn14 [17] and TNFα signaling through the TNFR-II [46] result in the degradation of cIAP1 and Traf2, ostensibly without affecting cIAP2. Baxter et al. [42] concluded that alternative NF-κB (p52) is a prosurvival transcription factor during mammary gland development. Thus, in the mammary gland, NF-κB (p52)-regulated cIAP2 may protect cells from rapid cell death induced by TNFα and Tweak thereby contributing to the reversibility of early stage involution.

The strong induction of P-Stat3 could contribute directly to cell death as described [29] and also indirectly induce Tweak [42]. Interestingly, recent evidence suggests that activation of Fn14 by Tweak can also activate Stat3 signaling [51] which

could establish a feedforward loop. The ensuing rapid cell death would be amplified by the absence of both cIAP1 and cIAP2 in the Tweak-stimulated *cIAP2*$^{-/-}$ mammary glands as described above.

Autophagy is thought to function as a short term survival mechanism during early involution [33, 42]. *cIAP2*$^{-/-}$ glands showed increased autophagic flux by d7.5 L coincident with the detection of numerous detached cells in the lumen of alveoli and ducts. Interestingly, Tweak has been demonstrated to promote anoikis of detached vascular smooth muscle cells [52]. The reduction in P-Erk1/2 may result from loss of attachment to the basement membrane while the expression of Bim at d19L is consistent with the early onset of anoikis since Bim is normally detected at late-stage involution [53]. The diminished level of P-Erk1/2 in *cIAP2*$^{-/-}$ mammary glands at 24hINV could also potentiate the pro-apoptotic effects of Stat3 in mammary glands [8]. Figure 7a summarizes the proposed role of cIAP2 in the mammary gland where cIAP2 contributes to prevention of mechanical stress-induced cell death during early involution.

IAP proteins are attractive targets for facilitating apoptosis in cancer cells, however, it is not clear whether cIAP1 and cIAP2 have redundant or distinct functions in tumor cell survival [54]. Human and mouse mammary tumors express NF-κB and inhibition prevents tumorigenesis [55, 56]. cIAP2 is robustly activated by NF-κB [57] and it is likely that cIAP2 survival signaling induced by NF-κB has a critical role in preventing cell death in transformed cells. In the DMBA/medroxyprogesterone (MPA) tumor model [45], MPA induces the RANKL/RANK axis in mammary epithelial cells and activation of NF-κB which then promotes proliferation, including DMBA-initiated cells [58]. The absence of cIAP2 in mammary tumors correlated with long latency associated with a high apoptotic rate. Nevertheless, tumors formed in *cIAP2*$^{-/-}$ mice at a similar frequency as in WT mice suggesting that proliferation eventually outpaces apoptosis in these tumors.

SMAC mimetics bind to cIAP1/2 proteins enhancing their E3 ligase activity to promote autoubiquitination resulting in the proteasomal degradation of cIAP1/2 proteins [59]. Since cIAPs restrain NF-κB activity, the degradation of cIAP1/2 induces cell death through NF-κB-mediated induction of TNFα [60, 61]. The extensive apoptosis in mammary tumors in the absence of cIAP2 indicates that cIAP1 does not fully compensate for this deficit which could be indicative of a general insufficiency in cIAP1/2 proteins and/or a discrete function of cIAP2 that is absent in the null mice. Indeed cIAP2 is more highly expressed in cancer cells than in normal tissue cells, due in part to activation by NF-κB [54]. Similar to the effects of SMAC mimetics, the reduction in overall levels of cIAP proteins in *cIAP2*$^{-/-}$ tunour cells could result in activation of the alternative NF-κB pathway, transcription of TNFα and induction of apoptosis pursuant to the deficit of cIAPs (Fig. 7b).

Results of the studies presented here demonstrate that cIAP2 has discreet cIAP1-independent roles in preventing rapid involution in the mammary gland and promoting survival during tumorigenesis.

Materials and Methods

Mice *cIAP2*$^{-/-}$ mice have been previously described [20]. Chimeric males were originally mated with 129/SvJ females then the heterozygous progeny were backcrossed to C57BL/6 mice for more than 10 generations. Genomic tail DNA was used for genotyping. Virgin female mice (C57BL/6 *cIAP2*$^{-/-}$ and WT controls) were sacrificed at 9 weeks of age. Virgin mice were communally caged but were not estrus matched based on vaginal smears. Pregnant and lactating mice (between the ages of 10–12 weeks) were sacrificed at different days after the appearance of a vaginal plug (days of pregnancy/dP) or after pups were born (days of lactation; dL) or after pups were removed (hours post-weaning/involution; hINV). Weaning took place on the morning of d21L or at d10L as indicated. Male mice were removed from the cages one day after appearance of the vaginal plug. Litters were monitored for suckling intermittently. The 4th inguinal mammary glands were removed and used for analysis. Three virgins/dams were analyzed in each experiment per time point.

DMBA/MPA-Induced Mammary Tumorigenesis *cIAP2*$^{-/-}$ females and WT littermates at 10 weeks of age were subcutaneously implanted dorsally with a 60-day medroxyprogesterone release pellet (Innovative Research, Hialeah, FL) and 5 days later began a course of gavages with 50 mg/kg DMBA in cottonseed oil [45]. Mice were monitored twice weekly for tumor formation by palpation following the final gavage of DMBA. All tumors were allowed to reach endpoint (maximum of 1cm^3). Three *cIAP2*$^{-/-}$ and two WT mice died without a palpable tumor within 60 days of final gavage. Tumors were removed immediately after euthanization of mice. Kaplan-Meier curves and statistics were generated based on time from last gavage to tumor endpoint using GraphPad Prism 4.0.

Animal housing and experimentation was conducted in accordance with the Canadian Council on Animal Care guidelines with the approval of the University of Ottawa animal care committee.

Mammary Gland Whole Mounts and Analysis Fourth inguinal mammary glands were excised from mice and spread onto glass microscope slides. Glands were fixed overnight in Carnoy's fixative (10% glacial acetic acid, 30% chloroform, 60% ethanol). Fixed glands were washed in 70%, 50%, 25% ethanol then distilled water for 15 min each then fat was extracted in acetone following 3–20 min incubations. Glands were rehydrated in 100% ethanol then 95% ethanol for

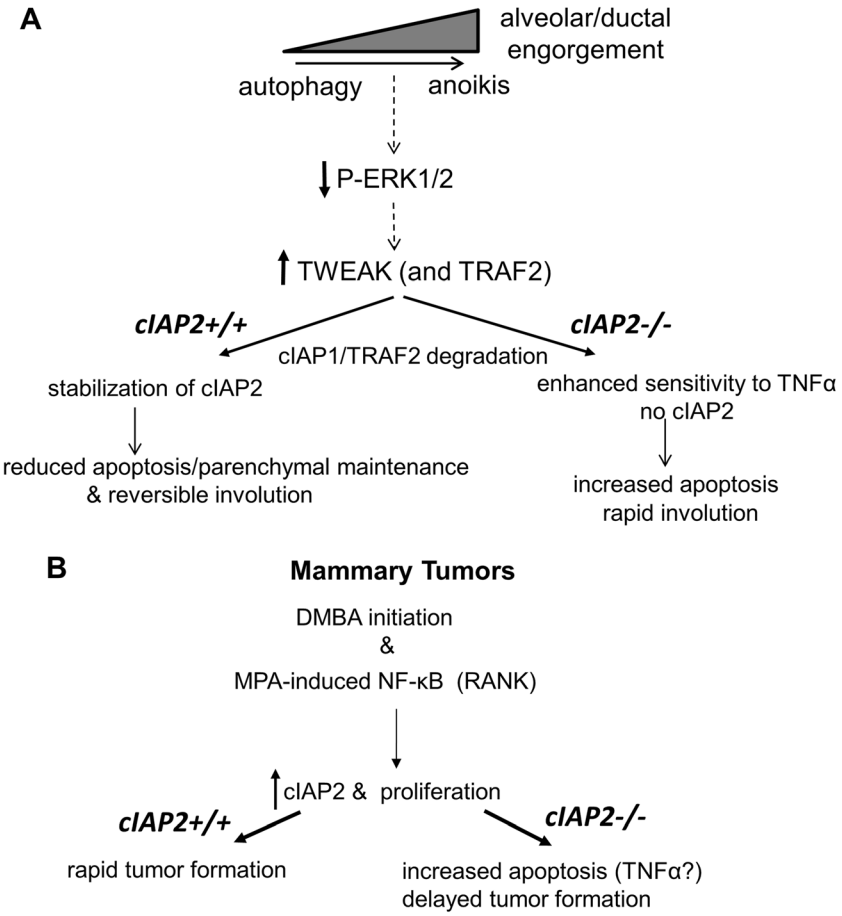

Fig. 7 Proposed roles of cIAP2 in the mammary gland. **a**, Alveolar and ductal stretch after weaning (or due to inadequate mammary branching complexity) results in myoepithelial detachment followed by luminal cell detachment or simultaneous separation of both cell layers from the basement membrane. Loss of attachment initiates autophagy which, when prolonged, leads to anoikis. The concerted cell detachment signals a proportionate induction of Tweak expression. In *cIAP2*$^{-/-}$ glands this results in accelerated involution, at least in part, due to the absence of cIAP2 which is stabilized in WT glands by reduced cIAP1 following its degradation induced by Tweak/Fn14. **b,** In the DMBA/MPA model of tumorigenesis MPA induces NF-κB through stimulation of RANKL thus promoting proliferation of carcinogen-initiated cells. NF-κB induces both TNFα and cIAP2 which promotes tumor cell survival in WT but not *cIAP2*$^{-/-}$ mouse mammary tumor cells where TNFα may contribute to apoptotic cell death

20 min each then stained with hematoxylin for one hour at room temperature. After rinsing clear in water, specimens were de-stained by submerging in acid alcohol (50% ethanol, 0.2% HCl) twice for 30 min and then in fresh acid alcohol overnight. Finally glands were dehydrated in 70%, 95 and 100% ethanol for 20 min each then stored in toluene. Samples were mounted using Permount (Fisher). Branch points were enumerated on the same duct relative to the nipple and lymph node on mammary glands from 3 different mice per genotype.

Immunoblots and Antibodies Total mammary gland and tumor protein extracts were obtained from snap frozen tissue that was pulverized under liquid N2. After the addition of RIPA buffer (50 mM Tris-HCl, 150 mM NaCl, 1% NP-40, 0.5% sodium deoxycholate, 0.1% SDS, pH 7.5, 10 μg/ml aprotinin, 1 μM pepstatin, 1 μM leupeptin, 1 mM phenylmethlysulfonyl fluoride (PMSF), 1 mM Na_2VO_4), the samples were sonicated then incubated on ice for 30 min. Insoluble material was removed by centrifugation at 9000 ***g*** for 20 min at 4 °C. Protein samples were aliquoted and frozen at -80C. Figures are representative of immunoblots of protein derived from at least two sets of mice of each genotype for each time point. Tumor samples were prepared in RIPA buffer and immunoblotting was performed as previously described [56]. The following primary antibodies were used for western blot analysis: anti-β-actin (Sigma #A-2066); anti-p38 #9212, anti-P-p38 #9211, anti-p100/p52 #4882, anti-Erk1/2 #4695, anti-P-Erk1/2 #9106, anti-STAT5 #9358, anti-P-STAT3 #9134, anti-STAT3 #9139, anti-caspase-3 #9661, anti-P-Akt ser473 #9271, anti-Akt #9272 (all from Cell Signaling), anti-P-STAT5 #562077 and anti-TRAF2 #558890 (BD Bioscience,); anti-vinculin (abcam, #ab129003); anti-LC3 (Novus Biologicals, #NB100–2220), anti-GAPDH (Biolegend, #MMS-5805); anti-BimEL (Millipore, #MAB17001), anti-β-casein (Santa Cruz Biotechnology #sc-166,520); anti-cIAP2 (Abcam #ab-23,423). Anti-rat

IAP1 (RIAP) was obtained from Dr. R. Korneluk. Both anti-IAP antibodies detect mouse cIAP1 and cIAP2 as previously described [9] (and supplemental references) and as per the Abcam datasheet. Where indicated, immunoblots were quantified using Image J2.

Mammary Gland and Tumor Sections Mouse tissues were paraffin-embedded and sections were prepared and stained with hematoxylin and eosin (H&E) using standard procedures by the University of Ottawa Department of Pathology and Laboratory Medicine. Briefly, slides were deparaffinized in toluene, hydrated (100%, 95%, 70% ethanol and water, 10 min each). Dehydration was performed in 70%, 95%, and 100% ethanol followed by toluene. H&E-stained sections were mounted with coverslips using permanent mounting media (Permount, Fisher). For immunohistochemistry, antigen retrieval was performed in the presence of 10 mM sodium citrate pH 6.0. Slides were blocked for 1 h in 2% normal goat serum, 1% BSA, 0.3% Triton-X-100. Anti-SMA or anti-p100/p52 antibody was diluted in antibody dilution buffer (DAKO #S0809) and incubated O/N at 4C followed by washing and the addition of DAKO Envision+peroxidase (DAKO K4002) and developed using DAB chromogen (DAKO) as per the manufacturer's instructions. Counter staining was performed using filtered hematoxylin followed by rinsing in distilled water. Dehydration was performed in 70%, 95 and 100% ethanol then toluene. Slides were mounted using Permount.

Densitometry and Statistics Densitometry was performed using open source Fiji/ImageJ2. Results were expressed as mean ± S.E.M. of three or more separate experiments. Student's t-test was used for statistical analysis. A p-value <0.05 was considered statistically significant.

qRT-PCR Mammary glands were stored in RNAlater (ThermoFisher Scientific). Total RNA was isolated using Tripure Isolation Reagent (Roche) or Qiazol (Qiagen) according to the manufacturer's protocol and was resuspended in 20 ul of nuclease-free water. cDNA was generated by reverse transcribing five μg of RNA with the RevertAid H Minus reverse transcriptase (Fermentas/ThermoFisher) or Superscript III (Invitrogen/ThermoFisher). The resulting cDNA was diluted 1:20 and used in a qRT-PCR reaction with FASTStart Universal SYBR Green Master Mix (Roche). All qRT-PCR reactions were performed with an ABI 7500 Real-Time PCR System (ABI/ThermoFisher) and relative gene expression was quantitated using the delta C_T method. Primers were designed online using the Roche Universal Probe Library Assay Design Center (https://lifescience.roche.com/shop/CategoryDisplay?catalogId=10001&tab=&identifier=Universal+Probe+Library) and manufactured by Invitrogen/ThermoFisher. Murine β-actin (*Actnb*) was used as the endogenous control for all experiments. Data shown is representative of 2 independent experiments performed in triplicate or the mean of values obtained from 3 mice for each time point as indicated in the figure legends.

Mouse Target Genes	Forward Primer	Reverse Primer
Actnb (beta-actin)	Ctaaggccaaccgtgaaaag	Accagaggcatacagggaca
Birc2 (*cIAP1*)	Gaagaaaatgctgaccctacaga	Aatgacgacatcttccgaac
Birc3 (*cIAP2*)	Tcgatgcagaagacgagatg	Tttgttcttccggattagtgc
Tnf	Ctgtagcccacgtcgtagc	Ttgagatccatgccgttg
Tweak	Caggatggagcacaagcag	Gctggagctgttgattttg

TUNEL Assays TUNEL assays were performed on paraffin sections of mammary tissue and tumors using the Millipore/Chemicon (Temecula, CA) Apoptag ® in situ apoptosis detection kit according to the manufacturer's directions.

Acknowledgements We thank Dr. Robert Korneluk for the generous gift of cIAP2-null mice and Drs. Eric Lacasse and Paul Hamel for helpful discussion. We thank Min Ying Niu for expert technical assistance. This work was supported by grants from the Canadian Institutes of Health Research grant FRN 79304 and the Canadian Breast Cancer Foundation, Ontario to M.A.C.P.

Compliance with Ethical Standards

Conflict of Interest The authors declare that they have no conflict of interest.

References

1. Watson CJ, Khaled WT. Mammary development in the embryo and adult: a journey of morphogenesis and commitment. Development. 2008;135:995–1003.
2. Asselin-Labat ML, Vaillant F, Sheridan JM, Pal B, Wu D, Simpson ER, et al. Control of mammary stem cell function by steroid hormone signalling. Nature. 2010;465:798–802.
3. Joshi PA, Jackson HW, Beristain AG, Di Grappa MA, Mote PA, Clarke CL, et al. Progesterone induces adult mammary stem cell expansion. Nature. 2010;465:803–7.
4. Schramek D, Leibbrandt A, Sigl V, Kenner L, Pospisilik JA, Lee HJ, et al. Osteoclast differentiation factor RANKL controls development of progestin-driven mammary cancer. Nature. 2010;468:98–102.
5. Lund LR, Rømer J, Thomasset N, Solberg H, Pyke C, Bissell MJ, et al. Two distinct phases of apoptosis in mammary gland involution: proteinase-independent and -dependent pathways. Development. 1996;122:181–93.
6. Li M, Liu X, Robinson G, Bar-Peled U, Wagner KU, Young WS, et al. Mammary-derived signals activate programmed cell death during the first stage of mammary gland involution. Proc Natl Acad Sci U S A. 1997;94:3425–30.
7. Clarkson RW, Wayland MT, Lee J, Freeman T, Watson CJ. Gene expression profiling of mammary gland development reveals putative roles for death receptors and immune mediators in post-lactational regression. Breast Cancer Res. 2004;6:R92–109.
8. Kritikou EA, Sharkey A, Abell K, Came PJ, Anderson E, Clarkson RW, et al. A dual, non-redundant, role for LIF as a regulator of

development and STAT3-mediated cell death in mammary gland. Development. 2003;130:3459–68.
9. Mahoney DJ, Cheung HH, Mrad RL, Plenchette S, Simard C, Enwere E, et al. Both cIAP1 and cIAP2 regulate TNFalpha-mediated NF-kappaB activation. *Proc Natl Acad Sci USA*. 2008;105:11778–83.
10. Hamanaka RB, Bobrovnikova-Marjon E, Ji X, Liebhaber SA, Diehl JA. PERK-dependent regulation of IAP translation during ER stress. Oncogene. 2009;28:910–20.
11. Bertrand MJ, Milutinovic S, Dickson KM, Ho WC, Boudreault M, Durkin J, et al. cIAP1 and cIAP2 facilitate cancer cell survival by functioning as E3 ligases that promote RIP1 ubiquitination. Mol Cell. 2008;30:689–700.
12. Silke J, Vucic D. IAP family of cell death and signaling regulators. Methods Enzymol. 2014;545:35–65.
13. Wang L, Du F, Wang X. TNF-alpha induces two distinct caspase-8 activation pathways. Cell. 2008;133:693–703.
14. Lin Y, Devin A, Rodriguez Y, Liu ZG. Cleavage of the death domain kinase RIP by caspase-8 prompts TNF-induced apoptosis. Genes Dev. 1999;13:2514–26.
15. Zarnegar BJ, Wang Y, Mahoney DJ, Dempsey PW, Cheung HH, He J, et al. Noncanonical NF-kappaB activation requires coordinated assembly of a regulatory complex of the adaptors cIAP1, cIAP2, TRAF2 and TRAF3 and the kinase NIK. *Nat Immunol* 2008; **9:** 1371–8
16. Saitoh T, Nakayama M, Nakano H, Yagita H, Yamamoto N, Yamaoka S. TWEAK induces NF-κB2 p100 processing and long lasting NF-κB activation. J Biol Chem. 2003;278:36005–12.
17. Vince JE, Chau D, Callus B, Wong WW, Hawkins CJ, Schneider P, et al. TWEAK-FN14 signaling induces lysosomal degradation of a cIAP1-TRAF2 complex to sensitize tumor cells to TNFalpha. J Cell Biol. 2008;182:171–84.
18. Ikner A, Ashkenazi A. TWEAK induces apoptosis through a death-signaling complex comprising receptor-interacting protein 1 (RIP1), Fas-associated death domain (FADD), and caspase-8. J Biol Chem. 2011;286:21546–54.
19. Silke J, Vaux DL. IAP gene deletion and conditional knockout models. Semin Cell Dev Biol. 2015;39:97–105.
20. Conte D, Holcik M, Lefebvre CA, Lacasse E, Picketts DJ, Wright KE, et al. Inhibitor of apoptosis protein cIAP2 is essential for lipopolysaccharide-induced macrophage survival. Mol Cell Biol. 2006;26:699–708.
21. Wright CW, Duckett CS. (2005). Reawakening the cellular death program in neoplasia through the therapeutic blockade of IAP function. J Clin Invest. 2005;115:2673–8.
22. Xu L, Zhu J, Hu X, Zhu H, Kim HT, LaBaer J, et al. c-IAP1 cooperates with Myc by acting as a ubiquitin ligase for Mad1. Mol Cell. 2007;28:914–22.
23. Annunziata CM, Davis RE, Demchenko Y, Bellamy W, Gabrea A, Zhan F, et al. Frequent engagement of the classical and alternative NF-kappaB pathways by diverse genetic abnormalities in multiple myeloma. Cancer Cell. 2007;12:115–30.
24. Keats JJ, Fonseca R, Chesi M, Schop R, Baker A, Chng WJ, et al. Promiscuous mutations activate the noncanonical NF-kappaB pathway in multiple myeloma. Cancer Cell. 2007;12:131–44.
25. DiDonato JA, Mercurio F, NF-kappaB KM. The link between inflammation and cancer. Immunol Rev. 2012;246:379–400.
26. Rinkenbaugh AL, Baldwin AS. The NF-κB pathway and Cancer stem cells. *Cells*. 2016;5:E16. https://doi.org/10.3390/cells5020016.
27. Owens TW, Foster FM, Tanianis-Hughes J, Cheung JY, Brackenbury L, Streuli CH. Analysis of inhibitor of apoptosis protein family expression during mammary gland development. BMC Dev Biol. 2010;10:71.
28. Olayioye MA, Kaufmann H, Pakusch M, Vaux DL, Lindeman GJ, Visvader JE. XIAP-deficiency leads to delayed lobuloalveolar development in the mammary gland. Cell Death Diff. 2005;12:87–90.
29. Kreuzaler PA, Staniszewska AD, Li W, Omidvar N, Kedjouar B, Turkson J, et al. Stat3 controls lysosomal-mediated cell death in vivo. Nat Cell Biol. 2011;13:303–9.
30. Beug ST, Beauregard CE, Healy C, Sanda T, St-Jean M, Chabot J, et al. Smac mimetics synergize with immune checkpoint inhibitors to promote tumour immunity against glioblastoma. Nat Commun. 2017; https://doi.org/10.1038/ncomms14278.
31. Cao Y, Bonizzi G, Seagroves TN, Greten FR, Johnson R, Schmidt EV, et al. IKKalpha provides an essential link between RANK signaling and cyclin D1 expression during mammary gland development. Cell. 2001;107:763–75.
32. Clarkson RW, Heeley JL, Chapman R, Aillet F, Hay RT, Wyllie A, et al. NF-kappaB inhibits apoptosis in murine mammary epithelia. J Biol Chem. 2000;275:12737–42.
33. Pensa S, Lloyd-Lewis B, Sargeant TJ, Resemann HK, Kahn CR, Watson CJ. Signal transducer and activator of transcription 3 and the phosphatidylinositol 3-kinase regulatory subunits p55α and p50α regulate autophagy in vivo. FEBS J. 2014;281:4557–67.
34. Ma Z, Liu Z, Myers DP, Terada LS. Mechanotransduction and anoikis: death and the homeless cell. Cell Cycle. 2008;7:2462–5.
35. Paoli P, Giannoni E, Chiarugi P. Anoikis molecular pathways and its role in cancer progression. Bio Biophys Acta. 2013;1833:3481–98.
36. Wen HC, Avivar-Valderas A, Sosa MS, Girnius N, Farias EF, Davis RJ, et al. p38α signaling induces Anoikis and lumen formation during mammary morphogenesis. Sci Signal. 2011;4(174):ra34.
37. Reginato MJ, Mills KR, Paulus JK, Lynch DK, Sgroi DC, Debnath J, et al. Integrins and EGFR coordinately regulate the pro-apoptotic protein Bim to prevent anoikis. Nat Cell Biol. 2003;5:733–40.
38. Ley R, Ewings KE, Hadfield K, Cook SJ. Regulatory phosphorylation of Bim: sorting out the ERK from the JNK. Cell Death Differ. 2005;12:1008–14.
39. Yun S, Vincelette ND, Knorr KL, Almada LL, Schneider PA, Peterson KL, et al. 4EBP1/c-MYC/PUMA and NF-κB/EGR1/BIM pathways underlie cytotoxicity of mTOR dual inhibitors in malignant lymphoid cells. Blood. 2016;127:271127–2.
40. Charvet C, Alberti I, Luciano F, Jacquel A, Bernard A, Auberger P, et al. Proteolytic regulation of Forkhead transcription factor FOXO3a by caspase-3-like proteases. Oncogene. 2003;22:4557–68.
41. Sargeant TJ, Lloyd-Lewis B, Resemann HK, Ramos-Montoya A, Skepper J, Watson CJ. Stat3 controls cell death during mammary gland involution by regulating uptake of milk fat globules and lysosomal membrane permeabilization. Nat Cell Biol. 2014;16:1057–68.
42. Baxter FO, Came PJ, Abel K, Kedjouar B, Huth M, Rajewsky K, et al. IKKbeta/2 induces TWEAK and apoptosis in mammary epithelial cells. Development. 2006;133:3485–94.
43. Scaffidi C, Medema JP, Krammer PH, Peter ME. FLICE is predominantly expressed as two functionally active isoforms, caspase-8/a and caspase-8/b. J Biol Chem. 1997;272:26953–8.
44. Hojilla CV, Jackson HW, Khokha R. TIMP3 regulates mammary epithelial apoptosis with immune cell recruitment through differential TNF dependence. PLoS One. 2011;6(10):e26718.
45. Aldaz CM, Liao QY, LaBate M, Johnston DA. Medroxyprogesterone acetate accelerates the development and increases the incidence of mouse mammary tumors induced by dimethylbenzanthracene. Carcinogenesis. 1996;17:2069–72.
46. Varfolomeev E, Goncharov T, Maecker H, Zobel K, Kömüves LG, Deshayes K, et al. Cellular inhibitors of apoptosis are global regulators of NF-κB and MAPK activation by members of the TNF family of receptors. Sci Signal. 2012;5(216):ra22.
47. Michaelson JS, Cho S, Browning B, Zheng TS, Lincecum JM, Wang MZ, et al. Tweak induces mammary epithelial branching morphogenesis. Oncogene. 2005;24:2613–24.
48. Voutilainen M, Lindfors PH, Lefebvre S, Ahtiainen L, Fliniaux I, Rysti E, et al. Ectodysplasin regulates hormone-independent

mammary ductal morphogenesis via NF-κB. *Preoc Natl Acad Sci U S A*. 2012;109:5744–9.

49. Liu Z, Li H, Wu X, Yoo BH, Yan SR, Stadnyk AW, et al. Detachment-induced upregulation of XIAP and cIAP2 delays anoikis of intestinal epithelial cells. Oncogene. 2006;25:7680–90.
50. Sherrill KW, Lloyd RE. Translation of cIAP2 mRNA is mediated exclusively by a stress-modulated ribosome shunt. Mol Cell Biol. 2008;28:2011–22.
51. Abell K, Bilancio A, Clarkson RW, Tiffen PG, Altaparmakov AI, Burdon TG, et al. Stat3-induced apoptosis requires a molecular switch in PI(3)K subunit composition. Nat Cell Biol. 2005;7(4): 392–8.
52. Wei B, Chen Z, Zhang X, Feldman M, Dong XZ, Doran R, et al. Nitric oxide mediates stretch-induced Ca2+ release via activation of phosphatidylinositol 3-kinase-Akt pathway in smooth muscle. PLoS One. 2008;3(6):e2526.
53. Schuler F, Baumgartner F, Klepsch V, Chamson M, Müller-Holzner E, Watson CJ, et al. The BH3-only protein BIM contributes to late-stage involution in the mouse mammary gland. Cell Death Differ. 2016;23:41–51.
54. LaCasse EC, Mahoney DJ, Cheung HH, Plenchette S, Baird S, Korneluk RG. IAP-targeted therapies for cancer. Oncogene. 2008;27:6252–75.
55. Cao Y, Luo JL, Karin M. IkappaB kinase alpha kinase activity is required for self-renewal of ErbB2/Her2-transformed mammary tumor-initiating cells. Proc Natl Acad Sci USA. 2007;104:15852–7.
56. Pratt MAC, Bishop TE, White D, Yasvinski G, Menard M, Niu MY, et al. Estrogen withdrawal-induced NF-kappaB activity and bcl-3 expression in breast cancer cells: roles in growth and hormone independence. Mol Cell Biol. 2003;23:6887–900.
57. Schoemaker MH, Ros JE, Homan M, Trautwein C, Liston P, Poelstra K, et al. Cytokine regulation of pro- and anti-apoptotic genes in rat hepatocytes: NF-kappaB-regulated inhibitor of apoptosis protein 2 (cIAP2) prevents apoptosis. J Hepatol. 2002;36:742–50.
58. Gonzalez-Suarez E, Jacob AP, Jones J, Miller R, Roudier-Meyer MP, Erwert R, et al. RANK ligand mediates progestin-induced mammary epithelial proliferation and carcinogenesis. Nature. 2010;468:103–7.
59. Fulda S. Promises and challenges of Smac mimetics as Cancer therapeutics. Clin Cancer Res. 2015;21:5030–6.
60. Varfolomeev E, Blankenship JW, Wayson SM, Fedorova AV, Kayagaki N, Garg P, et al. IAP antagonists induce autoubiquitination of c-IAPs, NF-kappaB activation, and TNFalpha-dependent apoptosis. Cell. 2007;131:669–81.
61. Vince JE, Wong WW, Khan N, Feltham R, Chau D, Ahmed AU, et al. IAP antagonists target cIAP1 to induce TNFalpha-dependent apoptosis. Cell. 2007;131:682–93.